JOURNAL OF BACTERIOLOGY, Aug. 1998, p. 4219–4226 Vol. 180, No. 16
0021-9193/98/$04.00+0

Phosphate Assimilation in *Rhizobium* (*Sinorhizobium*) *meliloti*: Identification of a *pit*-Like Gene

SYLVIE D. BARDIN, RALF T. VOEGELE, AND TURLOUGH M. FINAN*

Department of Biology, McMaster University, Hamilton, Ontario, Canada L8S 4K1

Received 10 September 1997/Accepted 1 June 1998

Rhizobium meliloti **mutants defective in the *phoCDET*-encoded phosphate transport system form root nodules on alfalfa plants that fail to fix nitrogen (Fix$^-$). We have previously reported that two classes of second-site mutations can suppress the Fix$^-$ phenotype of *phoCDET* mutants to Fix$^+$. Here we show that one of these suppressor loci (*sfx1*) contains two genes, *orfA* and *pit*, which appear to form an operon transcribed in the order *orfA-pit*. The Pit protein is homologous to various phosphate transporters, and we present evidence that three suppressor mutations arose from a single thymidine deletion in a hepta-thymidine sequence centered 54 nucleotides upstream of the *orfA* transcription start site. This mutation increased the level of *orfA-pit* transcription. These data, together with previous biochemical evidence, show that the *orfA-pit* genes encode a P_i transport system that is expressed in wild-type cells grown with excess P_i but repressed in cells under conditions of P_i limitation. In *phoCDET* mutant cells, *orfA-pit* expression is repressed, but this repression is alleviated by the second-site suppressor mutations. Suppression increases *orfA-pit* expression compensating for the deficiencies in phosphate assimilation and symbiosis of the *phoCDET* mutants.**

Because phosphate readily forms insoluble mineral phosphate complexes with other ions found in soil, the concentrations of soluble or available phosphate detected in soil solutions are low and generally range from 0.1 to 10 μM (3). While many *Rhizobium* strains are able to grow at these low phosphate concentrations (6), phosphate limitation often reduces dinitrogen fixation of legume-*Rhizobium* interactions by reducing both nodule number and mass (18, 26, 28). In addition, phosphate limitation may directly affect discrete steps during the nodule formation and infection process, such as excretion of Nod factors (22) and/or attachment to roots (17). Additional bacterial phenotypes of symbiotic importance which change in response to phosphate limitation include the biosynthesis and/or alteration of rhizobial cell surface carbohydrates such as exopolysaccharides II (45) and cyclic β-(1,2)-glucans in *Rhizobium meliloti* (5) and lipopolysaccharides in *Rhizobium leguminosarum* (32).

Our interest in phosphate metabolism in *R. meliloti* arose through our genetic analysis of the *ndvF* locus which is located on the pExo megaplasmid. The *ndvF* mutants form nodules on alfalfa that contain few bacteria and fail to fix N_2 (Fix$^-$) (8, 10). Two genetically distinct classes (I and II) of second-site mutations (*sfx*) which suppressed the *ndvF* Fix$^-$ phenotype were identified (25), and an analysis of those mutations together with a characterization of the *ndvF* locus has been the subject of several recent reports (1, 2, 37). The *ndvF* locus was shown to contain four genes, *phoCDET*, that encode an ABC-type high-affinity system for the uptake of phosphate and possibly phosphonates into the cell (2, 37). The *phoCDET* mutants were found to grow poorly in minimal media containing 2 mM orthophosphate (P_i) as a sole source of phosphorus (2). Class I suppressor mutations (*sfx1*, *sfx4*, and *sfx5*) are tightly linked in transduction, and we previously reported the localization of the *sfx1* locus to an 18-kb *Bam*HI fragment in the cosmid clone pTH56 (25). Here we show that *sfx1* possesses two genes, *orfA* and *pit*, and that the deduced Pit protein is homologous with phosphate transporters such as the Pit protein of *Escherichia coli*.

Analysis of class II suppressor mutations revealed that these mapped to the *phoU* and *phoB* regulatory genes and that disruption of these genes suppressed the Fix$^-$ and P_i growth phenotype of *phoCDET* (*ndvF*) mutants (1). We showed that while the *phoB* gene was required for expression of the *phoCDET* genes, *phoB* appeared to play a negative role in regulating expression of the *orfA-pit* genes. Here we demonstrate that the *sfx1* mutation is a promoter-up mutation which increases expression of the *orfA-pit* operon and allows P_i uptake via the OrfA-Pit system in a *phoCDET* mutant background. We conclude that this increased P_i uptake is responsible for the symbiotic phenotype associated with *phoCDET* mutations.

MATERIALS AND METHODS

Bacterial strains, plasmids, media, and growth conditions. The strains and plasmids used in this work are listed in Table 1. Transcriptional *lacZ* fusions to *pit* were made by subcloning the 2.1-kb *Eco*RI fragments from pTH354 (wild type) and pTH380 (*sfx1*) which included the *recF-orfA* intergenic region into the *Eco*RI site of the reporter plasmid pMP220 (31) to create plasmids pTH376 and pTH365, respectively. Transcriptional *lacZ* fusions to *orfA* were made by deleting the region between the *Sph*I site located in the *orfA* gene and the *Sph*I site of the pMP220 polylinker of plasmids pTH376 and pTH365 to create plasmids pTH378 and pTH367, respectively.

Plasmids pTH396 and pTH397 were constructed to delineate the fragment in which the *sfx1* mutation was located. Since the mutation was suspected to be in the promoter region, the 920-bp *Xho*I/*Eco*RI$_3$ and 540-bp *Eco*RV$_1$/*Eco*RI$_3$ fragments (*Eco*RI$_3$, for example, represents the *Eco*RI at the third site on the plasmid map; see Fig. 3) of pTH191 were subcloned as *Xho*I/*Hin*dIII and *Eco*RV/*Hin*dIII restriction sites of pBR322, respectively. The pBR322 vector was chosen because it is mobilizable by pRK600 but cannot replicate in *R. meliloti*. To provide a selectable marker to identify *R. meliloti* recombinants, the 3.4-kb *Hin*dIII fragment of pGS220 containing the Km^r gene of Tn*5* (12) was subcloned into the *Hin*dIII site of the two subclones.

The growth media used were Luria-Bertani medium (LB) and LB supplemented with 2.5 mM $MgSO_4$ and 2.5 mM $CaCl_2$ (LBmc) with antibiotic concentrations as previously described (8). The phosphate-free medium was the MOPS (morpholinepropanesulfonic acid)-buffered minimal medium described by Bardin et al. (1, 2) except that this medium was supplemented with a yeast extract fraction which stimulates growth of *R. meliloti* in defined medium (14 μl/liter) (41). For the growth experiments, strains grown for 24 h in LBmc were centrifuged and resuspended in phosphate-free MOPS medium (MOPS P0). Twenty microliters of the cells was used to inoculate 5 ml of MOPS P0 (optical density

* Corresponding author. Mailing address: Department of Biology, McMaster University, 1280 Main St. West, Hamilton, Ontario, Canada L8S 4K1. Phone: (905) 525-9140, ext. 22932. Fax: (905) 522-6066. E-mail: FINAN@MCMASTER.CA.

TABLE 1. Bacterial strains and plasmids

Strain or plasmid	Relevant characteristic(s)[a]	Reference
R. meliloti strains		
1021	SU47; *str-21*	14
Rm5408	ΔΩ5033-5007::Tn*5*-233 Fix$^-$	10
RmF263	ΔΩ5033-5007::Tn*5*-233 *sfx1* Fix$^+$	25
RmG203	ΔΩ5033-5007::Tn*5*-233 *sfx4* Fix$^+$	25
RmG204	ΔΩ5033-5064::Tn*5*-233 *sfx5* Fix$^+$	25
RmG212	*lac*	1
RmG439	ΔG439 (Δ*ndvF Hin*dIII::Nm^r [12 kb]) = *ndvF* ΔG439 Fix$^-$	10
RmG490	*ndvF*-1.7Ω Sp^r = *phoC*Ω490; Fix$^-$	10
RmG491	*ndvF*-5.3Ω Sp^r = *phoT*Ω491; Fix$^-$	10
RmG591	*sfx1*	25
RmG762	*phoC*Ω490 *sfx1* Fix$^+$	This work
RmG821	*phoC*Ω490 *sfx1* (*orf2*)*2*::Tn*5*	This work
RmG822	*phoC*Ω490 *sfx1 orfA23*::Tn*5*	This work
RmG830	*phoC*Ω490 *sfx1 pit10*::Tn*5* (same as *pit310*::Tn*5*)	This work
RmH138	*ndvF* Δ*G439 sfx1*	This work
RmH667	*lac phoC*Ω490	This work
RmH842	*phoC*Ω490 *sfx1 recF12*::Tn*phoA*	This work
Plasmids		
pUC118	Cloning vector; Ap^r	36
pRK600	pRK2013 *npt*::Tn*9* Cm^r Nm-Km^s	14
pRK7813	RK2 derivative carrying pUC9 polylinker and cos site; Tc^r	19
pGS220	Tn*5* in deletion derivative of pBR322; Ap^r Nm-Km^r	12
pMP220	IncP, promoterless *lacZ*; Tc^r	31
pTH56	pRK7813 clone carrying *sfx1*	25
pTH90	12-kb *Hin*dIII fragment of pTH56 in pRK7813, carrying *sfx1*	7
pTH191	2.1-kb *Eco*RI fragment of pTH90 in pUC118	This work
pTH276	4.8-kb *Hin*dIII/*Sac*I fragment of pTH90 in pRK7813	This work
pTH304	2.5-kb *Hin*dIII/*Sma*I fragment of pTH90 in pRK7813	This work
pTH305	2.6-kb *Hin*dIII/*Eco*RV fragment of pTH90 in pRK7813	This work
pTH347	2.6-kb partial *Eco*RI fragment of pTH90 in pRK7813 (ort I)	This work
pTH348	2.6-kb partial *Eco*RI fragment of pTH90 in pRK7813 (ort II)	This work
pTH354	4.8-kb *Hin*dIII/*Sac*I fragment in pUC118 isolated from wild-type genomic DNA and containing the wild-type *pit* allele	This work
pTH365	2.1-kb *Eco*RI fragment of pTH90 in pMP220; *sfx1* promoter *pit-lacZ* fusion	This work
pTH367	pTH365 Δ*Sph*I; *sfx1* promoter *orfA-lacZ* fusion	This work
pTH376	2.1-kb *Eco*RI fragment of pTH354 in pMP220; wild-type promoter *pit-lacZ* fusion	This work
pTH378	pTH376 Δ*Sph*I; wild-type promoter *orfA-lacZ* fusion	This work
pTH380	4.8-kb *Hin*dIII/*Sac*I fragment of pTH90 in pUC118	This work
pTH391	2.6-kb partial *Eco*RI fragment of pTH354 in pRK7813	This work
pTH396	0.9-kb *Hin*dIII-*Xho*I fragment of pTH191 in *Hin*dIII-*Sal*I sites of pBR322	This work
pTH397	0.6-kb *Hin*dIII-*Eco*RV fragment of pTH191 in *Hin*dIII-*Eco*RV sites of pBR322	This work

[a] Abbreviations: Ap, ampicillin; Cm, chloramphenicol; Gm, gentamicin; Km, kanamycin; Nm, neomycin; Sm, streptomycin; Sp, spectinomycin; Tc, tetracycline; *lac*, lactose utilization genes; ort I and II, orientations I and II (see Fig. 3); *oriV*, origin of vegetative replication.

at 600 nm [OD_{600}], ~0.05), and these cultures were grown for 24 h under agitation. This phosphate starvation step was necessary since, otherwise, significant growth occurred in MOPS P0 medium. The OD_{600} of the cultures was adjusted to 0.2, and 5-μl aliquots were used to inoculate 5 ml of MOPS P0 and 5 ml of MOPS supplemented with 2 mM P_i (MOPS P2). For the β-galactosidase assays, the LBmc-grown cells, supplemented with tetracycline at 2 μg/ml for the strains containing the pMP220-derived plasmids, were washed once with MOPS P0 and resuspended in this medium. Five-milliliter volumes of MOPS P0 and MOPS P2 were inoculated with 20 (OD_{600}, ~0.05) and 5 (OD_{600} ~0.015) μl of cells, respectively, and the cells were grown for 38 h before the assay was performed.

DNA manipulation and genetic techniques. Cloning procedures, including DNA isolation, restriction digestions, ligation, and transformation, were performed as described by Sambrook et al. (29). We cloned the wild-type *orfA-pit* region as a 4.8-kb *Hin*dIII-*Sac*I fragment from Rm1021 DNA into plasmid pUC118. One such plasmid, pTH354, was identified via colony hybridization by using a formamide-based hybridization solution at 42°C (described in reference 8) and a digoxigenin-labeled 4.8-kb *Hin*dIII-*Sac*I fragment from pTH90 as a probe. Annealed probe was detected with anti-digoxigenin antibody conjugated to alkaline phosphatase (AP).

Conjugal mating with MT616 as the helper strain, Tn*5* mutagenesis, and homogenizations (with pPH1JI) were performed as previously described (9, 13, 44).

DNA sequencing and sequence analysis. DNA sequencing of overlapping deletions was performed on single-stranded DNA by using the dideoxy chain termination method as described in the U.S. Biochemicals protocol for the Sequenase 2.0 enzyme and by using [α-^{35}S]ATP (NEN DuPont). Single-stranded DNA was obtained from host strain XL-1 Blue (Stratagene) following infection with the helper phage M13K07 (36). Both DNA strands were sequenced by using the −20 (*lacZ*) primer (5′-GTAAAACGACGGCCAGT-3′) and the IS50 primer (5′-TCACATGGAAGTCAGATCCT-3′). The *recF-orfA* intergenic region was amplified via the PCR by using primers 41, 5′-AAGTCGCTCAGTTTCAGGC GTGTGAGA-3′, and 55, 5′-CCCATGACGGTGCGCGAATGATCGG-3′ (see Fig. 4). Following gel purification, the sequences of the amplified 359- and 360-bp fragments were determined on an ABI automated DNA sequencer by using the above-described primer 41.

AP and β-galactosidase assays. The AP activity was measured as described by Yarosh et al. (44) except that the cells were centrifuged before the OD_{420} was measured. The AP activity was calculated by using the following formula: $(1{,}000 \times OD_{420})/(OD_{600} \times \Delta T)$, with ΔT being the reaction time (in minutes).

The β-galactosidase assay was performed, and specific activities in Miller units were calculated as previously described (1).

Determination of transcriptional start sites. Total RNA was isolated from MOPS P2 medium-grown cells by using the procedure outlined in the RNeasy Midiprep kit (Qiagen). Three different primers (primers 55, 81, and 82 [see Fig. 4]) were labeled with [γ-^{33}P]ATP (NEN Dupont) and polynucleotide kinase

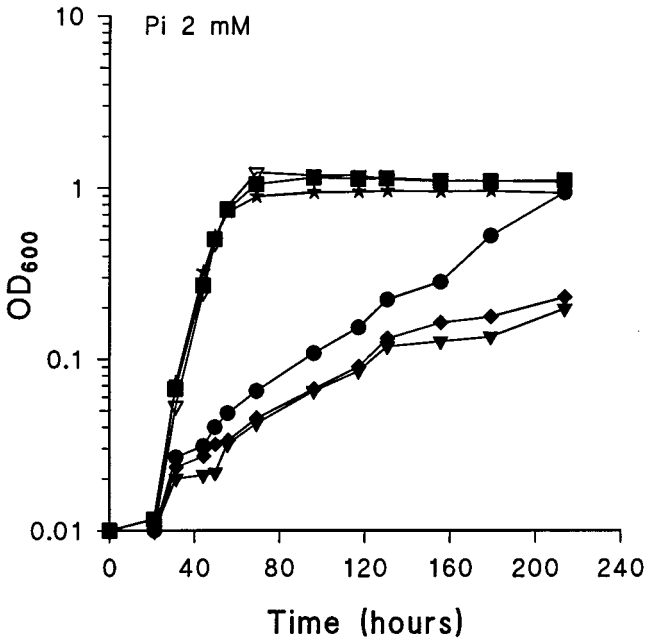

FIG. 1. Growth of Rm1021 (wild type) (■), RmG490 (*phoC*Ω490) (●), RmG762 (*phoC*Ω490 *sfx1*) (★), RmG822 (*phoC*Ω490 *sfx1 orf423*::Tn*5*) (◆), RmG830 (*phoC*Ω490 *sfx1 pit10*::Tn*5*) (▼), and RmH842 (*phoC*Ω490 *sfx1 recF12*::Tn*phoA*) (▽) in MOPS-buffered minimal medium supplemented with 2 mM P_i. Each time point represent the average of triplicate values. The growth curve for strain RmG821 [*phoC*Ω490 *sfx1* (*orf2*)*2*::Tn*5*] was similar to that for strain Rm1021, and the growth curves for *phoC*Ω490 *sfx1*::Tn*5* recombinants Ω16, -3, -J, -5, and -10A (Fig. 3) were similar to those for RmG822 and RmG830. In order to simplify the figure, these results are not shown.

(NEB). Thirty micrograms of RNA was annealed to labeled primer (4×10^5 to 1.5×10^6 cpm) and extended with Moloney murine leukemia virus reverse transcriptase for 90 min at 42°C. To align the transcriptional start sites, the same primers were used in conjunction with template DNA (pTH191, *sfx1*) in a standard sequencing reaction by using the Sequenase kit (Amersham, Oakville, Ontario, Canada).

Transport assays. For transport assays, cells were precultured in LBmc, washed three times with MOPS P0, and subcultured into MOPS P2. Cells grown aerobically for 24 h at 30°C were harvested by centrifugation, washed four times with MOPS P0, and resuspended to an OD_{600} of 10 in MOPS P0. Cells were diluted 1:20 into MOPS P0 and equilibrated for 5 min at 30°C. Uptake was initiated by the addition of [^{33}P]orthophosphoric acid (NEN DuPont) to a final concentration of 4 μM (175 Ci/mol). Aliquots were removed from the assay at different time points, placed on Millipore HAWP 02500 nitrocellulose filters (0.45-μm pore size; presoaked in 1 M K_2HPO_4-KH_2PO_4 [pH 7.0]), and immediately washed with 40 mM MOPS–20 mM KOH–20 mM NH_4Cl–100 mM NaCl–1.2 mM $CaCl_2$–2 mM $MgSO_4$. Filters were dried, placed in scintillation liquid (BCS; Amersham), and counted. All transport assays were performed in triplicate.

RESULTS

***sfx1* suppresses the P_i transport and growth phenotypes of *phoCDET* mutants.** Subsequent to the identification of *sfx1* as a second-site mutation which suppressed the Fix$^-$ symbiotic phenotype of *ndvF* mutants (25), we established that the *ndvF* locus contains four genes, *phoCDET*, which encode a phosphate transport system (2). Since *phoCDET* mutants grow slowly in medium containing 2 mM P_i and are defective in P_i transport (2), we wished to determine whether *sfx1* restored a wild-type growth and phosphate transport phenotype to *phoCDET* mutants.

Results from growth experiments showed that while the *R. meliloti phoC*Ω490 mutant, RmG490, grew slowly relative to the wild type, Rm1021, in medium containing 2 mM P_i, the doubling time for the *phoC*Ω490 *sfx1* strain, RmG762, was similar to that of the wild type (Fig. 1). Additional experiments revealed that *sfx1* also suppressed the slow-growth phenotype observed when either the *phoCDET* deletion (ΔG439) mutants or the *phoT*Ω491 insertion mutants were grown in MOPS–2 mM P_i (data not shown).

Measurements of the transport of ^{33}P-labeled inorganic phosphate into cells revealed that the rate of P_i uptake in the *phoC* mutant RmG439 was reduced relative to that of the wild type, Rm1021, whereas uptake into the *phoC sfx1* mutant strain, RmG762, was restored to the wild-type level (Fig. 2). Moreover, strain RmG830, which carries the *phoC*Ω490 mutation together with a Tn*5* insertion in the *sfx1* locus (*pit10*::Tn*5*), showed P_i uptake rates similar to those of the *phoC* mutant RmG490. These results established that the *sfx1* mutation restored wild-type phosphate transport and growth phenotypes to the *phoC* mutant. To further investigate the genetic nature of the *sfx1* locus, we first delineated the minimal gene region required for *sfx1*-mediated suppression.

Localization and nucleotide sequence of *sfx1*. The *sfx1* locus was previously located to the 18-kb *Bam*HI fragment on the pTH56 cosmid (25), and as a first step in the delineation of *sfx1*, a 12-kb *Hin*dIII fragment internal to the 18-kb region was subcloned into pRK7813 to give pTH90. This fragment contained the entire *sfx1* locus since RmG490 (*phoC*Ω490) pTH90 transconjugants formed Fix$^+$ nodules on alfalfa and grew like the wild-type strain in medium containing 2 mM phosphate (data not shown). Tn*5* insertions which mapped within the 12-kb insert of pTH90 were isolated, and seven of these plasmids were used to generate pTH90 deletion derivatives in which various amounts of the 12-kb insert region had been removed (Fig. 3, upper diagram). Fragments from the 12-kb region were also subcloned into pRK7813 (Fig. 3). The symbiotic Fix phenotype and/or phosphate growth phenotype of RmG490 (*phoC*Ω490) transconjugants carrying the various plasmids allowed us to deduce that the entire *sfx1* locus was located between the *Eco*RI_1 and *Eco*RV_1 sites indicated on the map of pTH276 in Fig. 3.

Transposon insertions within this region were recombined into the RmG762 (*phoC*Ω490 *sfx1*) chromosome (Fig. 3), and

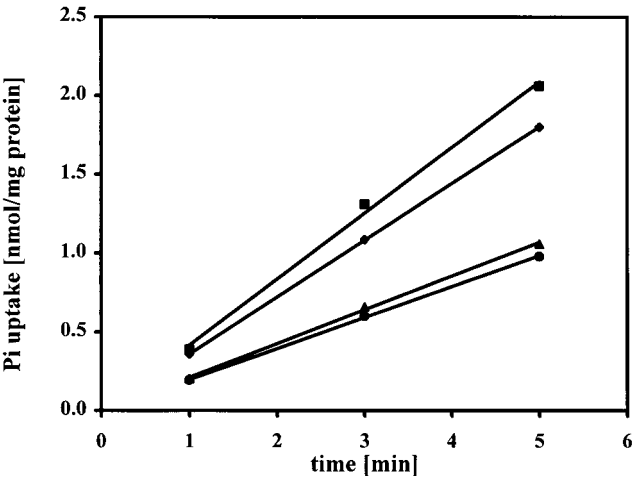

FIG. 2. P_i uptake in different *R. meliloti* mutants. [^{33}P]orthophosphoric acid was added to a final concentration of 4 μM. Results for *R. meliloti* Rm1021 (wild type) (◆), RmG490 (*phoC*Ω490) (▲), RmG762 (*phoC*Ω490 *sfx1*) (■), and RmG830 (*phoC*Ω490 *pit10*::Tn*5*) (●) are shown. The symbols represent the means of triplicate assays, and each line gives the linear regression for all data points for one strain. Background values for all strains were adjusted so that the results for the extrapolated zero time showed no P_i uptake.

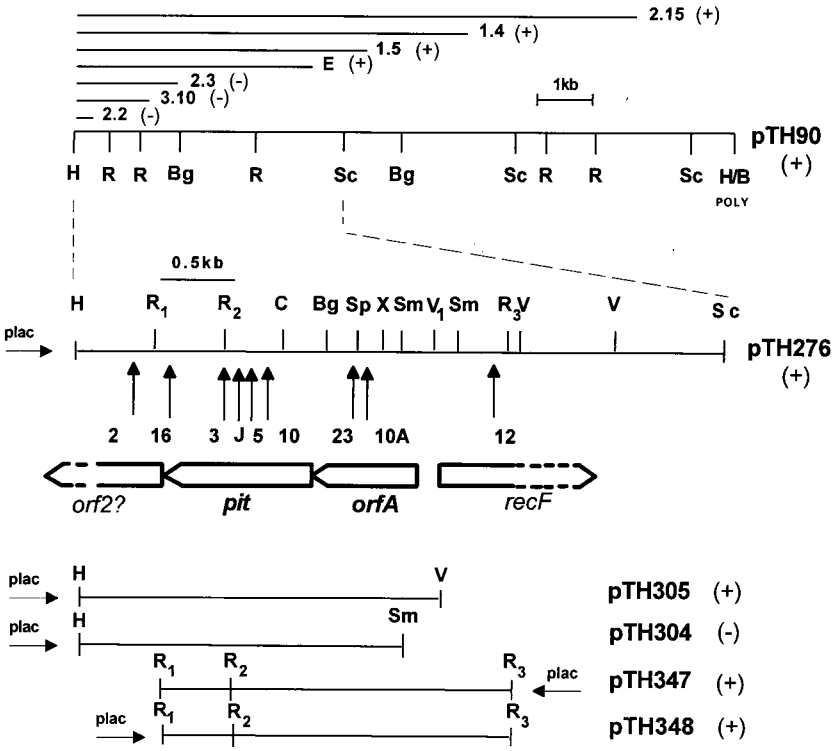

FIG. 3. Restriction maps of pTH90 and related plasmids. The upper diagram shows the regions which remained following deletion from the *Bam*HI site within Tn*5* transposons (Ω2.15, -1.4, -1.5, -E, -2.3, -3.10, and -2.2) to the *Bam*HI site in the polylinker of pTH90. Below the map for pTH276 are diagrammed the deduced *orfA-pit* genes and two partial *recF* and *orf2* open reading frames together with the Tn*5* insertions that disrupted the *sfx1* locus (Ω16, -3, -J, -5, -10, -23, and -10A) and the Ω2 and Ω12 insertions that did not. The orientation of fragments subcloned into pRK7813 are indicated relative to the position of the p*lac* promoter. The subclones are pTH276 (4.8-kb *Hin*dIII/*Sac*I), pTH305 (2.6-kb *Hin*dIII/*Eco*RV$_1$), pTH304 (2.5-kb *Hin*dIII/*Sma*I$_1$), and pTH347 and pTH348 (2.6-kb partial *Eco*RI in orientations I and II). The ability of the plasmids to suppress the Fix$^-$ and/or slow-growth phenotype of RmG490 (*phoC*Ω490) in MOPS P2 is indicated in parentheses (+, suppression; −, no suppression). Restriction site abbreviations: B, *Bam*HI; Bg, *Bgl*II; C, *Cla*I; H, *Hin*dIII; R, *Eco*RI; Sc, *Sac*I; Sm, *Sma*I; Sp, *Sph*I; V, *Eco*RV; X, *Xho*I. The subscripts following the R and V are used to specify particular sites.

the physical structure of the resulting recombinants was confirmed by Southern blot analysis (data not shown). The Ω2 and Ω12 recombinants grew like the suppressor strain RmG762 in MOPS medium containing 2 mM P_i, whereas the Ω16, -3, -J, -5, -10, -23, and -10A recombinants grew poorly (data not shown and Fig. 1). In addition, Ω10 and Ω23 recombinants formed Fix$^-$ nodules when tested on alfalfa plants (data not shown). These results confirmed that *sfx1* was located between the Ω2::Tn*5* insertion and the *Eco*RI$_3$ site. The nucleotide sequence of this 2,828-bp region was determined.

Analysis of the nucleotide sequence of the *sfx1* locus. Analysis of the nucleotide sequence revealed the presence of two complete open reading frames designated *orfA* and *pit* (see below) and (Fig. 3). The *orfA* stop codon (TGA) and the *pit* start codon (ATG) overlapped at the adenosine, suggesting that both genes are transcribed as a single transcript. The G+C contents of *orfA* and *pit* were 62 and 64%, respectively. There was a strong bias for G and C at the third position of the codons (83% for *orfA* and 87% for *pit*). This bias together with the codon usage of *orfA* and *pit* suggested that these genes were expressed in *R. meliloti* (24, 38).

A partial open reading frame initiating 234 bp upstream from *orfA* and whose 176-amino-acid product is homologous to the N-terminal regions of many RecF proteins, including *Caulobacter crescentus* (27), was detected (Fig. 3). An additional partial open reading frame (designated *orf2*), initiating 114 bp downstream of *pit*, was also found. Neither *recF* nor *orf2* was part of the *sfx1* locus since *recF*Ω12::Tn*5* and *orf2*Ω2::Tn*5* recombinants of strain RmG762 (*phoC*Ω490 *sfx1*) retained the suppressor phenotype (see above). An ATG start codon preceded by a potential ribosome binding site was found for each gene (CGGA-N6-ATG for *recF*, TGGA-N6-ATG for *orfA*, GAGA-N7-ATG for *pit*, and GAGA-N7-ATG for *orf2*).

GenBank searches (16) revealed that the 334-amino-acid *R. meliloti* Pit protein (RmPit) was similar in sequence to a large family of prokaryotic and eukaryotic phosphate transport proteins (42, 43; for a review, see reference 20), including the low-affinity Pit phosphate transport protein of *E. coli* (accession no. P37308; EcPitA) (30) and the phosphate-repressible phosphate permease of *Neurospora crassa* (accession no. P15710; NcPho-4$^+$) (21). In addition, RmPit showed similarity to numerous uncharacterized proteins, including the HI1604 protein of *Haemophilus influenza* (accession no. P45268) (15) and the EcPitB protein of *E. coli* (accession no. P43676) (4). Consistent with its homology to P_i transport proteins, an analysis of the RmPit sequence employing the TopPred II program (11) revealed nine "certain" membrane-spanning domains.

GenBank searches revealed that the 214-amino-acid OrfA protein had 21% amino acid identity with the deduced 226-amino-acid HI1603 protein of *H. influenzae* (accession no. P44271) (15). This result was interesting since the *HI1603* gene is located directly upstream (25 bp) from the *pit*-like *HI1604* gene of *H. influenzae* (see above). The conserved location of *orfA-pit*-like genes suggests that they are functionally related.

The *sfx1* mutation contains a single T deletion in a hepta-T sequence upstream of *orfA*. To investigate whether the *sfx1*

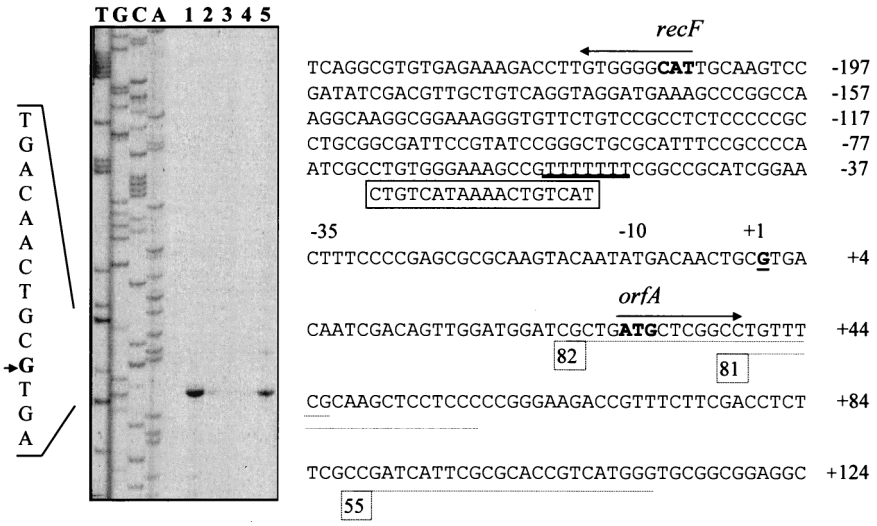

FIG. 4. Determination of the *orfA* transcriptional start sites. The autoradiograph shows the products of the sequencing reaction by using primer 55 and plasmid pTH191 (*sfx1*) as a template. The results for primers 81 and 82 yielded a start site identical to that with primer 55 (data not shown). The relevant sequence is shown on the left, and the arrow indicates the position of the extension product. Lane 1, RmG591 (*sfx1*) carrying pTH347 (*sfx1 orfA-pit* in orientation I); lane 2, RmG591; lane 3, Rm1021 (wild type); lane 4, Rm1021 carrying pTH391 (*orfA-pit*); lane 5, RmG591 carrying pTH348 (*sfx1 orfA-pit* in orientation II). The sequence on the right of the figure is the wild-type *recF-orfA* intergenic region. The deduced *orfA* transcriptional start site is in boldface type and underlined. The translational start sites for *orfA* and *recF* are in boldface type with arrows above indicating the direction of transcription. The three different primers used are indicated by thin underlines. The hepta-thymidine repeat is underlined, and a consensus PHO box sequence is shown below the putative PhoB-binding site. Numbers to the right of the sequence are nucleotide positions relative to the *orfA* transcriptional start site.

mutation lay in the *orfA-recF* intergenic region, the *Xho*I/*Eco*RI$_3$ and *Eco*RV$_1$/*Eco*RI$_3$ fragments from the *sfx1* locus (Fig. 3) in plasmids pTH396 and pTH397, respectively, were recombined via a Campbell-type single crossover into the RmG490 (*phoC*Ω490) genome (see Materials and Methods). The presence of the *sfx1* mutation was then determined by screening the recombinants for suppression of the mucoid colony phenotype of *phoCDET* mutants as observed on low-osmolarity GYM medium (25). Of 70 pTH396 recombinants examined, 12 formed dry colonies and thus suppressed the mucoid phenotype of RmG490. On the other hand, of 70 pTH397 recombinants examined, none showed a suppressor phenotype. Together, these data indicated that the *sfx1* mutation lay in the *orfA-recF* intergenic region.

The nucleotide sequence of the *Xho*I/*Eco*RV$_1$ fragments from the *sfx1* locus in pTH380 and the wild-type locus in pTH354 were determined. Both sequences were identical, except that a run of seven thymidines, present in the wild-type sequence at positions −80 to −86 upstream from *orfA*, was reduced to six thymidines in the *sfx1* mutant sequence (Fig. 4). A 359-bp fragment containing the complete *recF-orfA* intergenic region was PCR amplified from the wild type, Rm1021, and the two other class I suppressor strains, RmG203 (*sfx4*) and RmG204 (*sfx5*) (25). The nucleotide sequences of the amplified fragments revealed that all three were identical except that *sfx4* and *sfx5* mutant sequences, like the *sfx1* sequence, contained six thymidine residues in place of the seven thymidines present in the wild-type sequence. Thus, all three independently isolated class I suppressor mutants (*sfx1*, *sfx4*, and *sfx5*) carried the same thymidine deletion mutation. While this finding was surprising, we note that repeat sequences, such as the run of seven thymidines, are known to be mutational hot spots (23).

***sfx1* increases *orfA* and *pit* expression.** To investigate whether the *sfx1* mutation altered the level of *orfA-pit* expression, we constructed transcriptional *lacZ* fusions to the *orfA* and *pit* genes from both the wild-type and *sfx1* loci in the broad-host-range reporter plasmid pMP220 (see Materials and Methods). The resulting plasmids were transferred into the wild-type Lac$^-$ *R. meliloti* strain, RmG212, and the β-galactosidase (Fig. 5b) and AP (Fig. 5a) activities of the transconjugants were measured after 38 h of growth in MOPS-buffered medium containing either no phosphate (MOPS P0) or 2 mM inorganic phosphate (MOPS P2). High and low AP activities confirmed that the cells were grown under phosphate-deficient and phosphate-sufficient conditions, respectively (Fig. 5a, data sets 1, 2, and 4).

The results revealed, first, that both *pit* and *orfA* expression levels from the *sfx1* locus were three and five times higher, respectively, than expression from the wild-type locus (Fig. 5b, data sets 2 and 4). Second, *orfA* and *pit* expression was higher in cells cultured with excess P_i (MOPS P2) than in cells cultured with phosphate limitation (MOPS P0). Third, the level of *orfA* expression was three- to fivefold higher than the level of *pit* expression. In summary, the *sfx1* mutation increased the level of *orfA-pit* expression and both *sfx1*- and wild-type-directed expression appeared to be controlled via the phosphate concentration in the medium.

Since the *sfx1* mutation exerts its phenotypic effect in a *phoCDET* (*ndvF*) mutant background, we also measured both *orfA* and *pit* expression in a *phoC* Lac$^-$ background (RmH667). In this background, levels of both *orfA* and *pit* expression directed from the wild-type locus were very low regardless of whether the cells were cultured in the presence (2 mM) or absence of inorganic phosphate (Fig. 5b, data sets 3 and 5). On the other hand, while the expression of *sfx1-orfA* and *sfx1-pit* gene fusions was reduced by 23 to 30% in the *phoC* mutant relative to that in a wild-type background, their levels of expression were still two to three times higher than the levels of the corresponding wild-type fusions in a wild-type background. A two- to threefold increase in *orfA-pit* expression thus appears to be sufficient to allow suppression of the *phoCDET* phenotypes. We note that the high AP activity detected in *phoC* mutant cells cultured in medium containing 0 or 2 mM P_i suggests

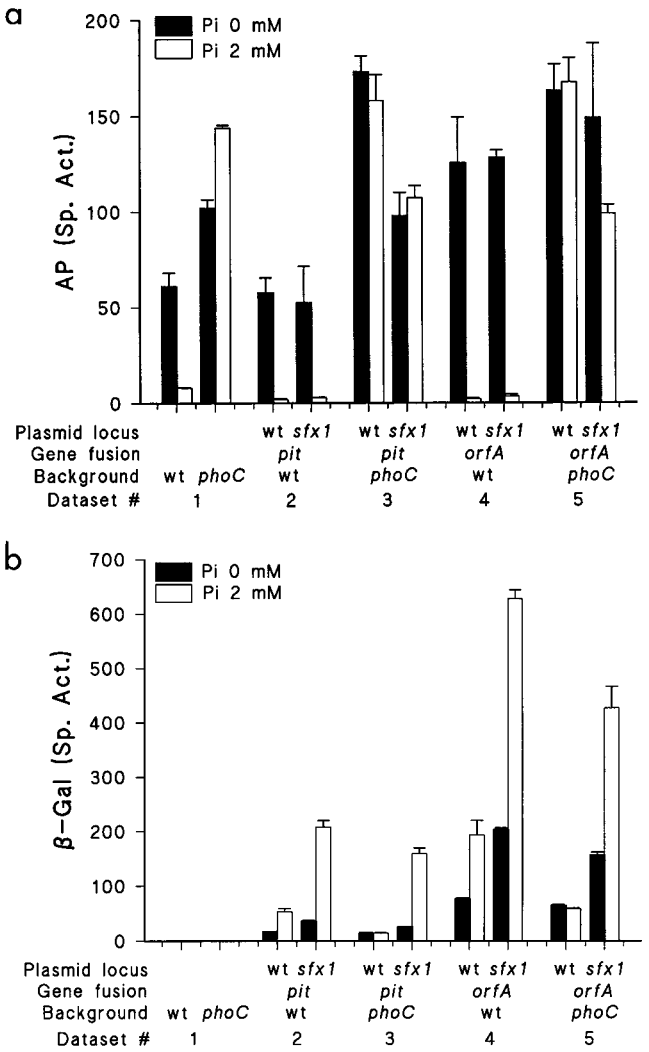

FIG. 5. Histogram showing AP (a) and β-galactosidase (b) activities from the *R. meliloti* wild type (wt), RmG212, and the RmG212 *phoC* mutant, RmH667. The strains represented in data sets 2 to 5 carried plasmid-borne *lacZ* gene fusions to the *pit* or *orfA* genes from the wild-type and *sfx1* loci, i.e., plasmids pTH376, pTH378, pTH365, and pTH367, respectively. Cells were assayed following 38 h of growth in MOPS-buffered minimal medium with no phosphate added (■) or supplemented with 2 mM phosphate (□). Each datum point represents the average of triplicate values ± standard error (error bar).

that these cells are starved for P_i (Fig. 5a, data sets 3 and 5) (see also reference 1).

The modest increase in *orfA-pit* transcription which resulted from the *sfx1* mutation prompted us to determine whether an increase in the copy number of the wild-type *orfA-pit* locus would be sufficient to allow the *phoC* mutant to grow in medium containing 2 mM P_i. The wild-type and *sfx1 orfA-pit* gene regions were therefore cloned into the broad-host-range vector pRK7813, and RmG490 (*phoC*) transconjugants carrying these plasmids (pTH391 and pTH348, respectively) grew like the wild-type strain, Rm1021, in MOPS P2 (data not shown). We therefore conclude that the increase in *orfA-pit* expression resulting from the increase in the copy number of the wild-type locus is sufficient to suppress the slow growth of the *phoC* mutant in medium containing 2 mM P_i.

The *orfA-pit* transcriptional start site lies 29 bp upstream of *orfA*. To investigate the relationship between the *sfx1* mutation and the *orfA-pit* promoter, we mapped the *orfA* transcriptional start site by primer extension analysis. mRNA was isolated from strains in which the copy numbers of the *sfx1* and wild-type *orfA-pit* regions were increased via the plasmids pTH391 and pTH348, respectively. A single transcriptional start site, lying 29 bp upstream from *orfA*, was identified with three separate primers (Fig. 4 and data not shown). The extension product observed from cells carrying additional copies of the wild-type *orfA-pit* gene region was much less intense than the product from cells carrying additional copies of the *sfx1* locus (Fig. 4, lanes 1, 4, and 5). Moreover, in strains carrying only the chromosomal copy of the *orfA-pit* gene region, a faint extension product was observed with mRNA isolated from *sfx1* strains while no product was detected in wild-type cells (Fig. 4, lanes 2 and 3). These results confirmed that the *sfx1* mutation increased *orfA* transcription, and the data also suggest that under growth conditions (2 mM P_i) in which the wild-type *orfA-pit* operon is maximally expressed, the actual level of transcription is low. These conclusions are consistent with the results from *lacZ* gene fusion studies described above.

We identified −10 and −35 consensus-like hexamers (TAT GAC and TTTCCC, respectively), followed by the hepta-thymidine repeat (−51 to −57), upstream from the transcriptional start site. Partially overlapping the heptathymidine repeat site of the *sfx1* mutation, we identified an 18-bp element which contained 11 bp identical to the consensus binding site for the *E. coli* PhoB protein (Fig. 4).

DISCUSSION

The data presented in this report and previous biochemical data (37) suggest that the *orfA-pit* operon of *R. meliloti* encodes a phosphate transport system whose expression is regulated by the amount of available inorganic phosphate. The *orfA-pit* genes are expressed in cells grown in the presence of excess phosphate (2 mM P_i), whereas under P_i limiting conditions *orfA-pit* transcription is repressed (Fig. 5). Unlike the latter wild-type pattern of *orfA-pit* regulation, our data show that in *phoCDET* mutant cells, transcription of the *orfA-pit* operon is repressed, even in cells cultured with excess P_i (2 mM) (Fig. 5b, data sets 3 and 5). Thus, *phoCDET* mutants grow poorly in medium containing 2 mM P_i and show a reduced P_i transport phenotype not because they lack the PhoCDET transport system but because *orfA-pit* expression is repressed. Hence, the P_i assimilation phenotypes resulting from *phoCDET* mutations are eliminated by secondary mutations such as *sfx1* which increase *orfA-pit* transcription. The fact that *sfx1* was identified as a suppressor of the Fix^- phenotype of *phoCDET* mutants reinforces the suggestion that the *phoCDET* Fix^- phenotype is a direct consequence of the P_i assimilation phenotype of these mutants.

In *E. coli* and *Acinetobacter johnsonii*, there is physiological evidence that a Pit-like phosphate transport system, which transports P_i as a neutral metal phosphate complex, operates during conditions of P_i excess and that under P_i limiting conditions a separate high-affinity phosphate transport system is employed for P_i uptake (PstSCAB in *E. coli*) (33–35, 39, 40). While the proposed role for the Pit protein in *R. meliloti* is similar to that of the *E. coli* Pit protein, our data clearly suggest that *orfA-pit* expression is phosphate regulated in *R. meliloti* whereas the *E. coli* Pit transport system is believed to be constitutively expressed (40).

Why *phoCDET* mutations result in repression of *orfA-pit* expression is unclear. However, we recently showed that this repression is mediated through the transcriptional activator PhoB since mutations which inactivate the *phoB* gene relieve

this repression (1). In wild-type cells, PhoB also appears to mediate the phosphate-dependent regulation of *orfA-pit* expression, since *orfA-pit* expression is constitutive in a *phoB* mutant background (1). In view of the above data, it is particularly interesting to find a PhoB-like binding site in the *orfA* promoter. In *E. coli*, genes whose expression is activated by PhoB contain a PhoB binding site in the −35 region of the promoter. Similarly, the *R. meliloti phoC* promoter contains a PhoB-like binding site in the −35 region, and *phoC* expression is positively regulated by *phoB* (2). The PhoB-like binding site of the *R. meliloti orfA-pit* wild-type promoter is centered at −62.5, and we suggest that this atypical positioning reflects the negative regulation of *orfA-pit* expression by PhoB.

While the single thymidine deletion (*sfx1*) mutation increases the basal expression and strength of the *orfA-pit* promoter, expression is still regulated by the level of available phosphate. Indeed, the *sfx1* mutation appears to increase the sensitivity of the *orfA-pit* promoter to regulation by phosphate, since *sfx1*-directed *orfA-pit* transcription was P_i regulated in both the wild-type and *phoC* backgrounds (Fig. 5b, data sets 2 to 5), whereas (as noted above) wild-type *orfA-pit* showed only very low expression in the *phoC* background (Fig. 5b, data sets 3 and 5). Given the location of the *sfx1* mutation and PhoB-like binding site (Fig. 4), it is not surprising that *sfx1* transcription is still subject to phosphate-dependent regulation. Further studies are clearly required to verify the PhoB binding site and to investigate how the deletion mutation increases the strength of the *orfA-pit* promoter.

ACKNOWLEDGMENTS

This work was supported by operating and strategic grants from the Natural Sciences and Engineering Research Council of Canada to T.M.F.

We thank Nathan Falcioni for technical assistance in identifying the *sfx3* and *sfx4* mutations, Bob Watson for the yeast extract fraction, and all members of the Finan laboratory for comments and discussions.

REFERENCES

1. **Bardin, S. D., and T. M. Finan.** 1998. Regulation of phosphate assimilation in *Rhizobium* (*Sinorhizobium*) *meliloti*. Genetics **148:**1689–1700.
2. **Bardin, S. D., S. Dan, M. Osteras, and T. M. Finan.** 1996. A phosphate transport system is required for symbiotic nitrogen fixation by *Rhizobium meliloti*. J. Bacteriol. **178:**4540–4547.
3. **Bieleski, R. L.** 1973. Phosphate pools, phosphate transport, and phosphate availability. Annu. Rev. Plant. Physiol. **24:**225–252.
4. **Bollinger, J. M., Jr., D. S. Kwon, G. W. Huisman, R. Kolter, and C. T. Walsh.** 1995. Glutathionylspermidine metabolism in *Escherichia coli*. Purification, cloning, overproduction, and characterization of a bifunctional glutathionylspermidine synthetase/amidase. J. Biol. Chem. **270:**14031–14041.
5. **Breedveld, M. W., A. L. Benesi, M. L. Marco, and K. J. Miller.** 1995. Effect of phosphate limitation on synthesis of periplasmic cyclic β-(1,2)-glucans. Appl. Environ. Microbiol. **61:**1045–1053.
6. **Cassman, K. G., D. N. Munns, and D. P. Beck.** 1981. Growth of *Rhizobium* strains at low concentrations of phosphate. Soil Sci. Soc. Am. J. **45:**520–523.
7. **Charles, T. C., and T. M. Finan.** Unpublished data.
8. **Charles, T. C., and T. M. Finan.** 1991. Analysis of a 1600-kilobase *Rhizobium meliloti* megaplasmid using defined deletions generated *in vivo*. Genetics **127:** 5–20.
9. **Charles, T. C., and T. M. Finan.** 1990. Genetic map of *Rhizobium meliloti* pRmSU47b. J. Bacteriol. **172:**2469–2476.
10. **Charles, T. C., W. Newcomb, and T. M. Finan.** 1991. *ndvF*, a novel locus located on megaplasmid pRmeSU47b (pExo) of *Rhizobium meliloti*, is required for normal nodule development. J. Bacteriol. **173:**3981–3992.
11. **Claros, M. G., and G. von Heijne.** 1994. TopPred II: an improved software for membrane protein structure predictions. Comput. Appl. Biosci. **10:**685–686.
12. **De Vos, G. F., G. C. Walker, and E. R. Signer.** 1986. Genetic manipulations in *Rhizobium meliloti* utilizing two new transposon Tn*5* derivatives. Mol. Gen. Genet. **204:**485–491.
13. **Finan, T. M., E. Hartwieg, K. Lemieux, K. Bergman, G. C. Walker, and E. R. Signer.** 1984. General transduction in *Rhizobium meliloti*. J. Bacteriol. **159:**120–124.
14. **Finan, T. M., B. Kunkel, G. F. De Vos, and E. R. Signer.** 1986. Second symbiotic megaplasmid in *Rhizobium meliloti* carrying exopolysaccharide and thiamine synthesis genes. J. Bacteriol. **167:**66–72.
15. **Fleischmann, R. D., M. D. Adams, O. White, R. A. Clayton, E. F. Kirkness, A. R. Kerlavage, C. J. Bult, J.-F. Tomb, B. A. Dougherty, J. M. Merrick, K. McKenney, G. Sutton, W. Fitzhugh, C. A. Fields, J. D. Gocayne, J. D. Scott, R. Shirley, L.-I. Liu, A. Glodek, J. M. Kelley, J. F. Weidman, C. A. Phillips, T. Spriggs, E. Hedblom, M. D. Cotton, T. R. Utterback, M. C. Hanna, D. T. Nguyen, D. M. Saudek, R. C. Brandon, L. D. Fine, J. L. Fritchman, J. L. Fuhrmann, N. S. M. Geoghagen, C. L. Gnehm, L. A. McDonald, K. V. Small, C. M. Fraser, H. O. Smith, and J. C. Venter.** 1995. Whole-genome random sequencing and assembly of *Haemophilus influenzae* Rd. Science **269:**496–512.
16. **Gish, W., and D. J. States.** 1993. Identification of protein coding region by database similarity search. Nat. Genet. **3:**266–272.
17. **Howieson, J. G., A. D. Robson, and M. A. Ewin.** 1993. External Pi and calcium concentrations and pH but not the product of rhizobial nodulation genes affect the attachment of *Rhizobium meliloti* to roots of annual medics. Soil Biol. Biochem. **25:**567–573.
18. **Israel, D. W.** 1993. Symbiotic dinitrogen fixation and host-plant growth during development of and recovery from phosphorus deficiency. Physiol. Plant. **88:**294–300.
19. **Jones, J. D. G., and N. Gutterson.** 1987. An efficient mobilizable cosmid vector, pRK7813, and its use in a rapid method for marker exchange in *Pseudomonas fluorescens* strain HV37a. Gene **61:**299–306.
20. **Kavanaugh, M. P., and D. Kabat.** 1996. Identification and characterization of a widely expressed phosphate transporter/retrovirus receptor family. Kidney Int. **49:**959–963.
21. **Mann, B. J., B. J. Bowman, J. Grotelueschen, and R. L. Metzenberg.** 1989. Nucleotide sequence of *pho-4*$^+$, encoding a phosphate-repressible phosphate permease of *Neurospora crassa*. Gene **83:**281–289.
22. **McKay, I. A., and M. A. Djordjevic.** 1993. Production and excretion of *nod* metabolites by *Rhizobium leguminosarum* bv. *trifolii* are disrupted by the same environmental factors that reduce nodulation in the field. Appl. Environ. Microbiol. **59:**3385–3392.
23. **Miller, J. H.** 1983. Mutational specificity in bacteria. Annu. Rev. Genet. **17:** 215–238.
24. **Muto, A., and S. Osawa.** 1987. The guanine and cytosine content of genomic DNA and bacterial evolution. Proc. Natl. Acad. Sci. USA **84:**166–169.
25. **Oresnik, I. J., T. C. Charles, and T. M. Finan.** 1994. Second site mutations specifically suppress the Fix$^-$ phenotype of *Rhizobium meliloti* mutations on alfalfa: identification of a conditional *ndvF*-dependent mucoid colony phenotype. Genetics **136:**1233–1343.
26. **Ribet, J., and J.-J. Drevon.** 1995. Increase in permeability to oxygen and in oxygen uptake of soybean nodules under limiting phosphorus nutrition. Physiol. Plant. **94:**198–304.
27. **Rizzo, M. F., L. Shapiro, and J. W. Gober.** 1993. Asymmetric expression of the gyrase B gene from the replication-competent chromosome in the *Caulobacter crescentus* predivisional cell. J. Bacteriol. **175:**6970–6981.
28. **Sa, T. M., and D. W. Israel.** 1991. Energy status and functioning of phosphorus-deficient soybean nodules. Plant Physiol. **97:**928–935.
29. **Sambrook, J., E. F. Fritsch, and T. Maniatis.** 1989. Molecular cloning: a laboratory manual, 2nd ed. Cold Spring Harbor Laboratory Press, Cold Spring Harbor, N.Y.
30. **Sofia, H. J., V. Burland, D. L. Daniels, G. Plunkett III, and F. R. Blattner.** 1994. Analysis of the *Escherichia coli* genome. V. DNA sequence of the region from 76.0 to 81.5 minutes. Nucleic Acids Res. **22:**2576–2586.
31. **Spaink, H. P., R. J. H. Okker, C. A. Wijffelman, E. Pees, and B. J. J. Lugtenberg.** 1987. Promoters in the nodulation region of the *Rhizobium leguminosarum* Sym plasmid pRL1JI. Plant Mol. Biol. **9:**27–39.
32. **Tao, H., N. Brewin, and K. D. Noel.** 1992. *Rhizobium leguminosarum* CFN42 lipopolysaccharide antigenic changes induced by environmental conditions. J. Bacteriol. **174:**2222–2229.
33. **van Veen, H. W., T. Abee, G. J. J. Kortstee, W. N. Konings, and A. J. B. Zehnder.** 1994. Translocation of metal phosphate via the phosphate inorganic transport (Pit) system of *Escherichia coli*. Biochemistry **33:**1766–1770.
34. **van Veen, H. W., T. Abee, G. J. J. Kortstee, W. N. Konings, and A. J. B. Zehnder.** 1993. Characterization of two phosphate transport systems in *Acinetobacter johnsonii* 210A. J. Bacteriol. **175:**200–206.
35. **van Veen, H. W., T. Abee, G. J. J. Kortstee, W. N. Konings, and A. J. B. Zehnder.** 1993. Mechanism and energetics of the secondary phosphate transport system of *Acinetobacter johnsonii* 210A. J. Biol. Chem. **268:**19377–19383.
36. **Vieira, J., and J. Messing.** 1987. Production of single-stranded plasmid DNA. Methods Enzymol. **153:**3–34.
37. **Voegele, R. T., S. Bardin, and T. M. Finan.** 1997. Characterization of the *Rhizobium* (*Sinorhizobium*) *meliloti* high- and low-affinity phosphate uptake systems. J. Bacteriol. **179:**7226–7232.
38. **Wada, K.-N., Y. Wada, F. Ishibashi, T. Gojobori, and T. Ikemura.** 1992. Codon usage tabulated from the GenBank genetic sequence data. Nucleic Acids Res. **20:**2111–2118.
39. **Wanner, B. L.** 1993. Gene regulation by phosphate in enteric bacteria. J. Cell. Biochem. **51:**47–54.

40. **Wanner, B. L.** 1996. Phosphorus assimilation and control of the phosphate regulon, p. 1357–1381. *In* F. C. Neidhardt, R. Curtiss III, J. L. Ingraham, E. C. C. Lin, K. B. Low, B. Magasanik, W. S. Resnikoff, M. Riley, M. Schaechter, and H. E. Umbarber (ed.), *Escherichia coli* and *Salmonella*: cellular and molecular biology, 2nd ed. ASM Press, Washington, D.C.
41. **Watson, R. W.** Personal communication.
42. **Willsky, G. R., and M. H. Malamy.** 1980. Characterization of two genetically separable inorganic phosphate transport systems in *Escherichia coli*. J. Bacteriol. **144:**356–365.
43. **Wilson, C. A., K. B. Farrell, and M. V. Eiden.** 1994. Properties of a unique form of the murine amphotropic leukemia virus receptor expression on hamster cells. J. Virol. **68:**7697–7703.
44. **Yarosh, O. K., T. C. Charles, and T. M. Finan.** 1989. Analysis of C_4-dicarboxylic acid transport genes in *Rhizobium meliloti*. Mol. Microbiol. **3:** 813–823.
45. **Zhan, H., C. C. Lee, and J. A. Leigh.** 1991. Induction of the second exopolysaccharide (EPSb) in *Rhizobium meliloti* SU-47 by low phosphate concentrations. J. Bacteriol. **173:**7391–7394.